An Enhancer Trap Screen for Ecdysone-Inducible Genes Required for Drosophila Adult Leg Morphogenesis

Julie Gates and Carl S. Thummel

Department of Human Genetics, Howard Hughes Medical Institute, University of Utah, Salt Lake City, Utah 84112-5331

Manuscript received June 8, 2000
Accepted for publication July 31, 2000

ABSTRACT

Although extensive studies of Drosophila imaginal disc development have focused on proliferation and patterning, relatively little is known about how the patterned imaginal discs are transformed into adult structures during metamorphosis. Studies focused primarily on leg development have shown that this remarkable transformation is coordinated by pulses of the steroid hormone ecdysone and requires the function of ecdysone-inducible transcription factors as well as proteases and components of the contractile cytoskeleton and adherens junctions. Here, we describe a genetic screen aimed at expanding our understanding of the hormonal regulation of Drosophila adult leg morphogenesis. We screened 1300 lethal *P*-element enhancer trap insertions on the second chromosome for a series of sequential parameters including pupal lethality, defects in leg morphogenesis, and ecdysone-induced *lacZ* reporter gene expression. From this screen we identified four mutations, one of which corresponds to *bancal*, which encodes the Drosophila homolog of hnRNP K. We also identified *vulcan*, which encodes a protein that shares sequence similarity with a family of rat SAPAP proteins. Both *bancal* and *vulcan* are inducible by ecdysone, thus linking the hormone signal with leg morphogenesis. This screen provides new directions for understanding the hormonal regulation of leg development during Drosophila metamorphosis.

EPITHELIAL morphogenesis is the driving force behind many of the central processes of development including gastrulation, neurulation, and organogenesis. We are studying the metamorphic development of the leg imaginal discs of Drosophila in an effort to understand the basic mechanisms that underlie epithelial morphogenesis.

Imaginal discs are small epithelial sacs that give rise to specific portions of the adult integument (epidermis and cuticle) including the adult appendages. They are formed during embryogenesis as invaginations of the embryonic ectoderm. During larval development, the imaginal discs proliferate and are spatially patterned, resulting in each cell acquiring a position and fate in the adult structure (Cohen 1993). The appendage-forming imaginal discs are then transformed from an essentially flat layer of cells to mature adult structures by sequential high-titer pulses of the steroid hormone 20-hydroxyecdysone (hereafter called ecdysone; Fristrom and Fristrom 1993). The pulse of ecdysone at the end of larval development triggers disc morphogenesis as it signals puparium formation and the prepupal stage of development. During the first 6 hr after puparium formation, the leg and wing imaginal discs elongate to obtain the general shape of the adult appendages and evert to the outside of the animal. This is followed by fusion of the discs to create a continuous epidermal layer. Approximately 12 hr after puparium formation, a second pulse of ecdysone signals the prepupal-pupal transition and triggers inflation of the leg and wing discs. Inflation is proposed to result from contraction of the abdominal muscles and leads to the sudden extension of the appendages to their final length (Fristrom and Fristrom 1993). Following inflation, the leg and wing imaginal discs undergo additional rounds of proliferation, final shape refinements, and differentiation of hairs and bristles, resulting in mature adult appendages. The imaginal discs provide an ideal and simple model system in which to study epithelial morphogenesis as they are easily isolated, their responses to ecdysone in culture mimic their responses *in vivo*, and their development has proven amenable to molecular genetic analysis (von Kalm *et al.* 1995). We have focused our studies of epithelial morphogenesis on the elongation of the leg imaginal disc, which has been extensively characterized both *in vivo* and in culture by Fristrom and colleagues.

The late third instar leg imaginal disc consists of a concentrically folded single layer of epithelial cells. For this disc to assume the form of an adult leg it must telescope out along the proximodistal axis and constrict along its circumference. Remarkably, this dramatic morphological transformation occurs in the absence of proliferation and is driven by changes in cell shape (Condic *et al.* 1991). These cell shape changes are thought to result from contraction of the apical contractile belt that encircles each cell near its apical edge. The apical contractile belt is composed of actin and nonmuscle

Corresponding author: Carl Thummel, Department of Human Genetics, HHMI, University of Utah, 15 N. 2030 East, Rm. 5100, Salt Lake City, UT 84112-5331. E-mail: carl.thummel@genetics.utah.edu

myosin and is attached to the inner surface of the cell at intercellular adherens junctions. The involvement of the apical contractile belt in this process is supported by the observation that cytochalasins (agents that disrupt actin filaments) reversibly inhibit leg elongation in culture (Fristrom and Fristrom 1975). For cells to respond to the force exerted by the apical contractile belt, their attachments to the extracellular matrix layers that cover the apical and basal surfaces of the disc must be severed. This separation appears to be achieved through the action of proteases, as the addition of trypsin to prepupal leg discs in culture has been shown to accelerate elongation, while the addition of protease inhibitors blocks this process (Fekete *et al.* 1975). A role for proteases during leg disc elongation is further supported by the observation that prepupal leg discs make and secrete proteases in response to ecdysone in culture (Poodry and Schneiderman 1971; Fekete *et al.* 1975; Pino-Heiss and Schubiger 1989).

Failure of the leg imaginal disc cells to change shape during prepupal development results in discs that are not fully elongated and malformed adult legs with short, thick segments (Beaton *et al.* 1988; Condic *et al.* 1991; Gotwals and Fristrom 1991; von Kalm *et al.* 1995). This malformed leg phenotype has been used to identify a number of genes that are required for leg elongation, including those that encode both structural and regulatory proteins. Among the genes that mediate cell shape changes are *zipper* (*zip*; Gotwals and Fristrom 1991; Fristrom and Fristrom 1993), *spaghetti squash* (*sqh*; Edwards and Kiehart 1996), *daschous* (*ds*; Clark *et al.* 1995), and *Stubble* (*Sb*; Beaton *et al.* 1988). The subunits of Drosophila nonmuscle myosin II are encoded by *zip* (Young *et al.* 1993) and *sqh* (Edwards and Kiehart 1996). As expected, these proteins localize to the apical contractile belt where they, in conjunction with actin, are responsible for generating the contractile forces necessary for leg elongation. *ds* encodes a member of the cadherin superfamily and is a putative component of the adherens junction (Clark *et al.* 1995). On the basis of its homology to vertebrate cadherins, Ds is proposed to function in maintaining proper cell-cell adhesion and in the transmission of contractile forces across the epithelium (Geiger and Ayalon 1992). *Sb* encodes an apparent type II transmembrane serine protease that is localized to the apical surface of imaginal disc cells. It is proposed to function by severing the attachments between the cell and the apical extracellular matrix, thereby facilitating cell shape changes (Appel *et al.* 1993).

Consistent with a role for ecdysone as a critical signal for leg morphogenesis, mutations in ecdysone-induced regulatory genes can also lead to a malformed leg phenotype. These genes include the *Broad-Complex* (*BR-C*; Kiss *et al.* 1988), *E74* (Fletcher *et al.* 1995), β*FTZ-F1* (Broadus *et al.* 1999), and *crooked legs* (*crol*; D'Avino and Thummel 1998), all of which encode families of related transcription factors. These genes are thought to coordinate the expression of downstream secondary-response genes that mediate the cell shape changes associated with leg elongation. The *BR-C* consists of three genetically separable functions. One of these, the *broad* function, is essential for leg disc elongation as the leg imaginal discs fail to elongate in strong loss-of-function *broad* mutants (Kiss *et al.* 1988). In addition, the *BR-C* has proven to be a valuable tool for the identification of other genes that function during this process. Screens for mutations that dominantly enhance a weak hypomorphic *broad* allele, $broad^{1}$, led to the identification of *zip* and *Sb* (Beaton *et al.* 1988; Gotwals and Fristrom 1991). *Sb* expression is also induced by ecdysone (Appel *et al.* 1993). This suggests that ecdysone triggers leg disc elongation by inducing the expression of both structural and regulatory genes that direct this response.

crol mutations were identified in a small scale screen of lethal *P*-element insertion lines that were examined for their ability to meet a series of criteria, including a prepupal or pupal lethal phase, a malformed leg mutant phenotype, and defects in ecdysone-regulated gene transcription (D'Avino and Thummel 1998). The success of this screen prompted us to expand our search to allow the identification of structural as well as regulatory genes. To achieve this goal, we screened a collection of lethal *P*-element *lacZ* enhancer trap lines for a series of phenotypes, including a prepupal and/or pupal lethal phase, a malformed leg mutant phenotype, and *lacZ* reporter gene expression consistent with regulation by ecdysone. Using this approach, we identified mutations in four genes that function during leg elongation. Among these genes are *bancal*, which encodes the Drosophila homologue of heterogeneous nuclear ribonucleoprotein K (hnRNP K), and *vulcan*, which encodes a protein related to SAP-90/PSD-95 associated proteins (SAPAPs).

MATERIALS AND METHODS

Fly stocks: The second chromosome lethal *P*-element insertion lines used in our screen were kindly provided by the Berkeley *Drosophila* Genome Project (BDGP) and are available either through the Bloomington Stock Center or the BDGP (Spradling *et al.* 1995, 1999). *l(2)05271* and *l(2)07022* were generated from the mutagenesis described by Karpen and Spradling (1992) while *l(2)k08305* and *l(2)k10209* were generated by Torok *et al.* (1993). *Df(2R)M41A4* was obtained from the Bloomington Stock Center. $bancal^{w5}$ was provided by S. Kerridge and *dlg* alleles were provided by P. Bryant.

Phenotypic characterization: Each *P*-element insertion was balanced over a *CyO* y^{+} chromosome in a *y w* background. Animals homozygous for the *P*-element insertion were identified by the yellow phenotype of their mouth hooks and dentical belts. For all experiments, *y w* animals were used as the control. When necessary, animals were maintained on food containing 0.1% bromophenol blue and third instar larvae were staged as described (Andres and Thummel 1994).

Lethal phase analysis: The degree of embryonic lethality

caused by each mutation was determined by collecting embryos from the cross *yw*; P(w^+ or ry^+)/*CyO* y^+ × *yw*; P(w^+ or ry^+)/*CyO* y^+. For the control, embryos were collected from the cross: *yw*; +/*CyO* y^+ × *yw*; +/*CyO* y^+. The total number of embryos was counted and placed at 25°. After 2 days, the number of dead embryos was counted. To determine the lethality caused by each mutation during later stages of development, embryos were collected from the above cross and allowed to hatch. Homozygous mutant first instar larvae were selected on the basis of the yellow phenotype of their mouthhooks and dentical belts and maintained at a density of 50 animals/vial on fresh yeast paste and standard culture media that had been scored. The vials were placed at 25° and the number of pupae were counted after 4–5 days. Any difference between the observed number of pupae and 50 was presumed to represent the number of animals that died as larvae. The remaining pupae were examined daily and the number of animals dying as prepupae, early pupae, or pharate adults was determined. Any mutant animals that eclosed were placed in fresh vials and observed until their death. The percentage of animals dying as adults refers to animals that die within 2–3 days of eclosing from their pupal case.

Histochemical staining for β-galactosidase: Staged mid-third instar larvae (−18 hr relative to puparium formation) and late third instar larvae (−4 hr relative to puparium formation) were dissected in PBS and fixed in 4% formaldehyde in PBS for 3 min. After rinsing two to three times in PBS, organs were incubated in staining solution [150 mM NaCl, 1 mM $MgCl_2$, 3.3 mM $K_4(Fe[CN]_6)$, 3.3 mM $K_3(Fe[CN]_6)$, 10 mM sodium phosphate pH 7, 0.1% triton] containing a saturating amount of X-Gal for 16–20 hr at 37°. The stained organs were then rinsed two to three times in PBS. Following an overnight incubation in 50% glycerol in PBS at 4°, the imaginal discs were dissected, mounted, and photographed using a Zeiss Axiophot microscope.

Organ culture: To determine if *lacZ* reporter gene expression is induced by ecdysone, staged mid-third instar larvae were placed into oxygenated Grace's insect cell culture medium (GIBCO BRL, Gaithersburg, MD) and bisected. The posterior half of the larvae was discarded and the anterior half was turned inside out to expose the organs. The gut and fat body were then removed, leaving the brain and imaginal discs attached to the larval cuticle. These imaginal disc complexes were cultured in the presence of oxygen for 16 hr as described previously (Andres and Thummel 1994), with the exception that Grace's medium was used instead of Robb's medium. Half of the disc complexes were cultured with 5×10^{-6} M 20-hydroxyecdysone (Sigma, St. Louis) while the other half were cultured with an equal amount of ethanol (the solvent for the hormone stock). Following culture, the disc complexes were fixed and stained for β-galactosidase expression as described above.

Northern blot hybridizations: RNA was isolated from staged control and homozygous mutant animals by direct phenol extraction as previously described (Andres and Thummel 1994). Equal amounts of RNA from each stage were fractionated by formaldehyde agarose gel electrophoresis and transferred to a nylon membrane (Genescreen; Dupont, Wilmington, DE) as described (Karim and Thummel 1991). A probe to detect *vulcan* transcription was generated by PCR amplification of bases 720–1260 from the cDNA LD18846. A probe to detect *bancal* transcription was generated by PCR amplification of bases 103–720 from the cDNA GM13955. The DNA fragments generated by PCR were gel purified (Geneclean; BIO 101, Vista, CA) and labeled by random priming (Prime-It kit; Stratagene, La Jolla, CA). The blots were hybridized, washed, and stripped as described (Karim and Thummel 1991).

RESULTS

Identification of mutations in four genes required for leg morphogenesis: Our screen focused on the second chromosome, where the BDGP had collected 1300 lethal *P*-element insertion lines (Spradling *et al.* 1999). These *P*-element-induced mutations offer several advantages, including established methods to move from mutation to gene and the presence of a *lacZ* reporter gene within the *P* element that can be used to assay expression of the mutated gene. To identify mutations in genes that are regulated by ecdysone and required for leg morphogenesis, we screened for four parameters: (1) prepupal and/or pupal lethality, (2) malformed adult legs, (3) induction of *lacZ* expression *in vivo* in parallel with the late larval ecdysone pulse, and (4) induction of *lacZ* expression by ecdysone in cultured organs. We used these criteria to sequentially reduce the number of lines from 1300 to 4.

We initially screened for prepupal and/or pupal lethality to focus our efforts on mutations that cause defects in leg morphogenesis. To determine which lines met this criterion, vials of flies were allowed to age for 3 wk at room temperature after which the sides of the vials were examined for dead pupae. Lines that revealed ≥10% dead pupae were retained. Using this approach, a total of 148 lines were selected for further analysis. This collection was further refined to 37 lines by selecting stocks in which malformed adult legs could be seen through the pupal case.

We next took advantage of the *lacZ* reporter gene in the *P*-element insertion by determining whether there is a temporal correlation between *lacZ* expression and the late larval pulse of ecdysone. This allowed us to focus our efforts on genes that might be induced by the ecdysone pulse that triggers the initial stages of leg eversion and elongation. To determine which of the 37 lines met this criterion, imaginal discs were dissected from both mid-third instar larvae, when the ecdysone titer was low, and late third instar larvae, when the ecdysone titer peaked, and stained for *lacZ* expression (Figure 1). A total of 12 lines displayed a significant increase in *lacZ* expression at the end of larval development, and one line displayed a decrease, consistent with regulation by ecdysone.

The analysis of *lacZ* expression patterns described above provides a temporal correlation between *lacZ* expression and ecdysone titer. While this suggests that the mutated genes are regulated by ecdysone, we wanted to verify hormonal regulation by assaying whether the expression of the mutated gene could be induced by ecdysone in cultured imaginal discs. Imaginal discs were dissected from mid-third instar larvae, cultured in the absence or presence of ecdysone for 16 hr, and stained for *lacZ* expression. Of the 12 lines examined, 4 revealed little or no *lacZ* expression in the absence of ecdysone and a high level of *lacZ* expression in the presence of

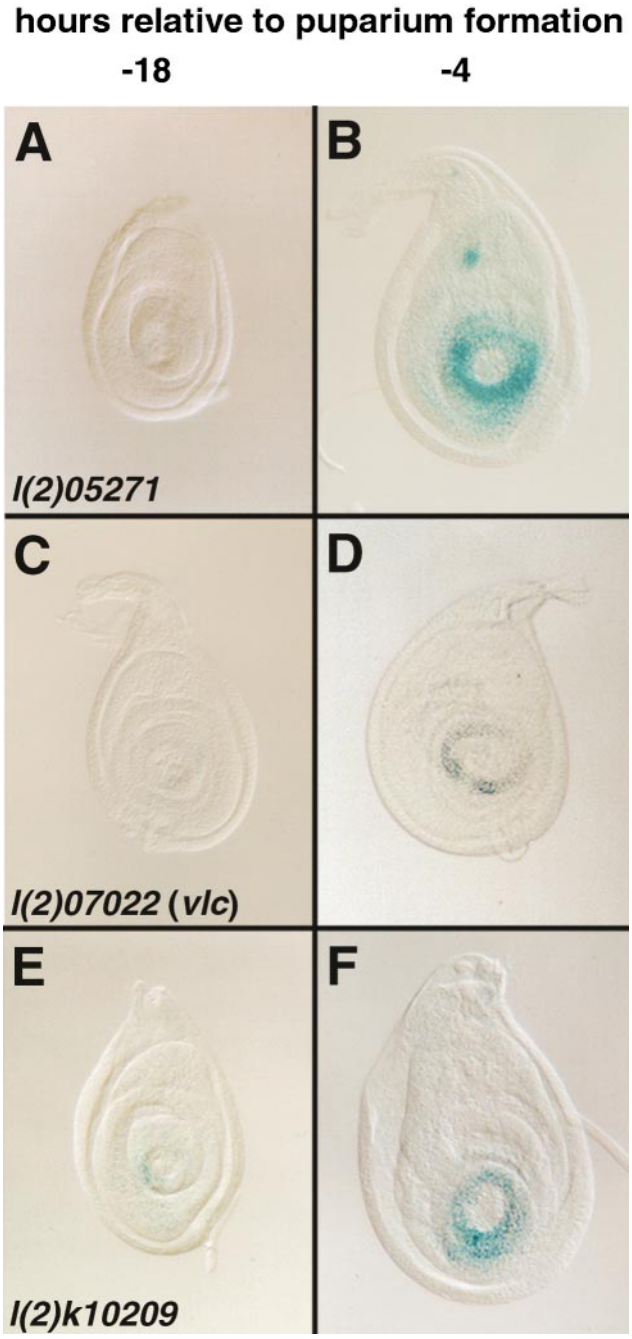

FIGURE 1.—*lacZ* expression in enhancer trap lines is induced in parallel with the late larval ecdysone pulse. Leg imaginal discs were dissected from mid-third instar larvae (−18 hr relative to puparium formation) and late third instar larvae (−4 hr relative to puparium formation) and stained for *lacZ* expression. Shown here are the *lacZ* expression patterns in leg imaginal discs for three of the four lines isolated in the screen. The spatial and temporal *lacZ* expression pattern of line *l(2)k08305* is identical to that of line *l(2)05271* and is therefore not shown.

the hormone, similar to that seen in staged animals (data not shown). Having met all of our criteria, we then characterized these 4 lines in more detail. These lines are designated *l(2)05271*, *l(2)07022*, *l(2)k08305*, and *l(2)k10209*.

Mutant animals from three out of the four lines die primarily during metamorphosis: We first characterized the lethal phases associated with each of the four selected mutations to determine whether this would reveal earlier essential functions. To assess embryonic lethality, a collection of embryos was obtained from a cross between flies heterozygous for each *P*-element insertion and a *CyO* balancer chromosome, and the number of dead embryos was determined. Since 25% of the embryos are homozygous for the balancer chromosome and are expected to die (Table 1, control), the percentage of dead embryos observed must be significantly >25% to indicate lethality caused by the mutation. Only one of the lines, *l(2)k10209*, revealed a substantial amount of embryonic lethality, with 45% of the embryos dying (Table 1). The other three lines revealed little or no embryonic lethality.

In an effort to identify later lethal phases, homozygous mutant first instar larvae were selected from each of the four lines and followed throughout development. Line *l(2)k10209* revealed significant lethality during all stages examined, suggesting that the corresponding gene is required throughout development (Table 1). Line *l(2)05271* displayed 16% lethality during larval development, suggesting that the corresponding gene performs some essential functions prior to metamorphosis. However, the majority of the lethality associated with this line, as well as the lethality associated with *l(2)07022* and *l(2)k08305*, was during early pupal and pharate adult stages (Table 1). Interestingly, some homozygous mutant adult flies were able to eclose in lines *l(2)05271*, *l(2)k08305*, and *l(2)k10209*, but these adults died 2 to 3 days later. These mutants fall into two general classes: (1) animals with severely malformed legs that are unable to inflate their wings and (2) animals with wild-type legs and wings that are approximately the same size as control wings, but which appear broader along the anterior/posterior axis (data not shown). Because the broad wing phenotype is often associated with malformed legs (GOTWALS and FRISTROM 1991; VON KALM *et al.* 1995), the identification of these two classes of adult escapers provides further support for a role for these genes during leg and wing morphogenesis.

Mutant animals display a malformed leg phenotype: A central criterion of our screen was that the mutation results in malformed legs. This was initially scored by examining intact mutant late pupae or pharate adults. At this stage the bristles have differentiated and the cuticle has become pigmented, making the identification of the appendages unambiguous. In control animals, the legs are positioned along the ventral surface and extend to the posterior tip of the abdomen in an organized manner (Figure 2A). In contrast, the legs of mutant animals display a range of phenotypes, from failing to extend to the tip of the abdomen but remaining organized (Figure 2E) to being both short and bent (Figure 2, B–D) or curved around the edge of the

TABLE 1

Lethal phase analysis

	N	Embryo (%)	*N*	Larva (%)	Prepupa (%)	Early pupa (%)	Pharate adult (%)	Adult (%)
Control	440	25	100	1	2	3	3	0
l(2)05271	123	31	147	16	1	16	37	30
l(2)07022 (*vlc*)	98	33	98	1	1	14	84	0
l(2)k08305 (*bl*)	106	27	97	5	2	12	35	46
l(2)kl10209	251	45	148	38	3	32	21	6

Two separate experiments were used to determine the lethal phases of the mutant animals. To determine the degree of embryonic lethality caused by each mutation, embryos were collected from the cross *yw*; P(w^+ or ry^+)/*CyO* y^+ × *yw*; P(w^+ or ry^+)/*CyO* y^+ and the percentage of dead embryos determined. For the control, embryos were collected from the cross *yw*; +/*CyO* y^+ × *yw*; +/*CyO* y^+. *N* refers to the total number of eggs collected. To determine the lethality caused by each mutation during later stages of development, homozygous mutant first instar larvae from the above cross were selected and their development monitored. *N* indicates the total number of mutant larvae examined. The percentage of animals dying as adults refers to animals that die within 2–3 days of eclosing from their pupal case. *yw* animals were used as the control.

wing (Figure 2, C and D). The wings also appear to be affected in some of the mutant animals, failing to extend as far down the body as the wings of control animals (Figure 2C). The severity of this phenotype, however, is difficult to assess as the wings are highly folded at this stage. In contrast to the appendage-forming imaginal discs, the development of the imaginal histoblast nests seems unaffected as the abdomens of the mutant late pupae appear normal.

To more carefully determine the nature of the leg phenotype, third legs were dissected from representative mutant pharate adults and examined in more detail (Figure 3). Third legs were chosen as they are almost always the most severely affected leg and, in some animals, the only legs that display a phenotype. In all cases, mutant legs contain the appropriate number of segments with the appropriate identity, but the shape of some segments is abnormal. In animals displaying the classic malformed leg phenotype, segments of the leg, especially the femur and tibia and often the basi-tarsus, are shorter and thicker than normal (von Kalm *et al.* 1995). The femur, tibia, and basi-tarsus of most of the mutant legs examined were either short and thick (Figure 3, B and D basi-tarsi) or misshapen, containing constrictions (Figure 3, D and E femurs) or bends (Figure 3B tibia, 3C tibia and 2nd tarsal). These defects thus closely correspond to the malformed leg phenotype defined by Fristrom and colleagues (Beaton *et al.* 1988; Gotwals and Fristrom 1991; von Kalm *et al.* 1995).

The malformed leg phenotype is first evident during prepupal development: To determine when the malformed leg phenotype arises, we examined leg imaginal discs from mutant third instar larvae and prepupae. The overall morphology and size of late third instar mutant discs is indistinguishable from imaginal discs dissected from control animals (data not shown). Furthermore, the expression patterns of both Distal-less (Panganiban *et al.* 1995) and Cubitus interruptus proteins (Motzny and Holmgren 1995) in mutant late third instar imaginal discs are identical to those seen in wild-type animals (data not shown). On the basis of these criteria, we conclude that the mutant imaginal discs have been properly patterned during larval development.

Figure 2.—Legs of mutant pharate adults are short and misshapen. Shown here are control and representative homozygous mutant pharate adults for each of the four enhancer trap lines studied. These animals have been fixed and removed from their pupal case to make it easier to see the leg phenotype. The legs of control animals extend the full length of the abdomen in an organized manner (A). The legs of the mutant animals display a range of phenotypes from failing to extend to the tip of the abdomen but remaining organized (E) to being both short and bent (B–D) or curved around the edge of the wing (C and D). Apparent differences in the relative sizes of mutant pharate adults are not reproducible.

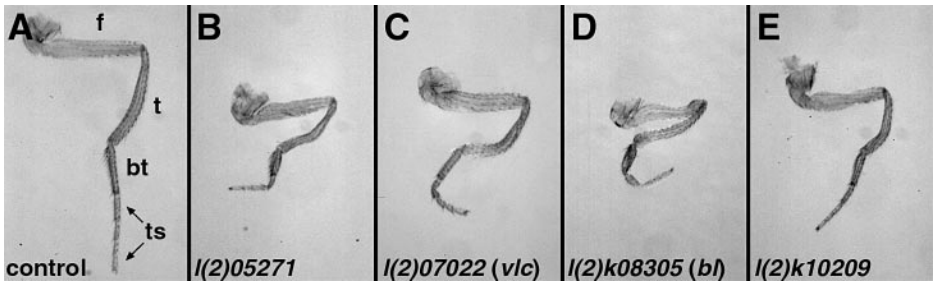

FIGURE 3.—Mutant legs are malformed. Third legs were removed from control and representative homozygous mutant pharate adult animals. All legs examined were found to contain the proper number of segments with the proper identity, but the segments were often misshapen. Some of the segments are kinked (femur in D and E), while others are shorter and thicker than normal (basi-tarsus in B and D) or are bent (second tarsal segment in C). f, femur; t, tibia; bt, basi-tarsus or first tarsal segment; ts, second through fifth tarsal segments with the fifth tarsal segment being the most distal.

Leg elongation is complete by 6 hr after puparium formation, resulting in discs that had taken on the general shape of an adult leg (FRISTROM and FRISTROM 1993). To determine if mutant leg imaginal discs are able to complete elongation normally, we examined the morphology of leg discs from mutant animals at 6–8 hr after puparium formation. Because the elongated imaginal discs are quite fragile at this stage in development, we examined disc morphology through the pupal case of intact animals, thus avoiding mounting artifacts that might result from dissection. At least a portion of the mutant midprepupae from each of the four lines displayed malformed legs, ranging from 14 to 91% of the population, suggesting that the malformations observed in these animals are the result of a defect in leg disc elongation (Table 2). However, an increased number of pupae and adults of lines *l(2)05271*, *l(2)07022*, and *l(2)k08305* display malformed legs relative to the frequency of malformed legs seen in midprepupae (Table 2). This suggests that either the midprepupal malformed phenotype is not evident in some animals until later in development or that morphogenetic events during pupal development contribute to the malformed phenotype in these mutants.

Determination of whether the *P*-element insertion is responsible for the malformed leg phenotype: *P*-element insertion lines can contain second-site mutations, making it necessary to establish that the phenotype observed is caused by the *P* insertion. Three methods can be used to demonstrate this connection: reversion of the phenotype by precise excision of the *P* element, free recombination to remove second-site mutations, and examination of animals heterozygous for the *P* element and a deficiency that spans the insertion site. Using these methods we were able to determine that two out of the four lines isolated in our screen contain second-site mutations that are responsible for both the lethality and malformed leg phenotype.

For line *l(2)05271*, we generated nearly 100 excision events and were unable to recover any that resulted in reversion of the malformed leg and lethal phenotypes. Furthermore, all animals heterozygous for *l(2)05271* and each of six deficiencies that collectively span ~1600 kb around the insertion site were viable and fertile with no obvious defects. We were able to confirm the insertion site reported by the BDGP by matching genomic DNA sequence with that flanking the *l(2)05271 P* element, thereby excluding the possibility that the *P* element was inserted outside of the reported cytogenetic interval. Taken together, these data indicate that the phenotype of *l(2)05271* is not due to the *P*-element insertion.

For line *l(2)k10209*, we generated 65 excision events and were also unable to recover any that resulted in

TABLE 2

Penetrance of malformed leg phenotype

	N	% of midprepupae with malformed leg(s)	*N*	% of pupae and adults with malformed leg(s)
Control	40	3	100	1
l(2)05271	20	65	122	97
l(2)07022 (*vlc*)	21	14	96	27
l(2)k08305 (*bl*)	24	46	94	78
l(2)k10209	22	91	87	94

The percentage of mutant animals with at least one malformed leg was determined in midprepupae and animals from later stages. For midprepupae and pupae, the morphology of the legs was examined through the pupal case of intact animals. Legs were considered to be malformed if they either failed to extend as far down the pupal case as legs of control animals or were bent. For *l(2)05271*, *l(2)k08305*, and *l(2)k10209*, a portion of the mutant animals eclosed from their pupal case; legs were considered to be malformed if any of the segments were kinked, bent, or shorter and thicker than normal. *yw* animals were used as the control.

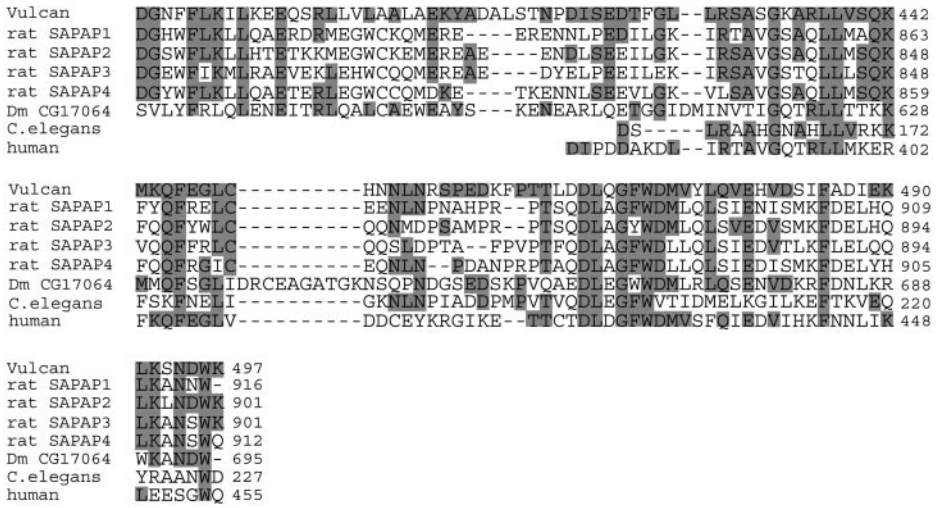

FIGURE 4.—A region of the Vulcan protein shares identity with the family of rat SAPAP proteins. Shown is a sequence comparison between the amino acid sequence of the predicted Vulcan protein and that of the rat SAPAP proteins over a region of 115 amino acids near the carboxy terminus of Vulcan (TAKEUCHI *et al.* 1997). Also shown are alignments with proteins of unknown function predicted from Drosophila (Dm CG17064), *C. elegans*, and human sequences (GenBank accession nos. AAF58367, U00058, and D13633, respectively). Amino acids that are identical between Vulcan and at least one of the other proteins are shaded.

reversion of the malformed leg and lethal phenotypes. Additionally, we carried out free recombination with this line. We established seven lines for which we followed the w^+ eye marker contained within the *P* element through three generations of single female matings to w^{1118} males. The seven recombined chromosomes were then placed over balancer chromosomes and animals homozygous for the *P*-element insertion were analyzed. In three of these lines, animals carrying a homozygous *P*-element insertion were viable and fertile with no obvious phenotype. These results indicate that a second-site mutation present on the original chromosome is responsible for the phenotypes associated with line *l(2)k10209*. This conclusion has been recently confirmed by the BDGP (SPRADLING *et al.* 1999). It is important to note, however, that although the phenotypes of lines *l(2)05271* and *l(2)k10209* are not due to the *P*-element insertion, they still contain mutations in genes that result in malformed legs and therefore are of interest to our work. Our future plans include efforts to map these mutations and identify the mutated gene in these lines.

For line *l(2)07022* we generated 14 excision events, none of which resulted in reversion of the malformed leg or lethal phenotypes. This is not surprising, however, as we later determined that this *P* element is inserted within the coding region of a gene. In addition, animals heterozygous for *l(2)07022* and *Df(2R)M41A4*, a deficiency that spans ~740 kb around the *P*-element insertion site, display the same phenotype as animals homozygous for *l(2)07022*. This indicates that the mutant phenotype is attributable to the *P*-element insertion in line *l(2)07022*.

For line *l(2)k08305* we generated 65 excision events, 49 of which resulted in complete reversion of the mutant phenotype. We also examined animals heterozygous for *l(2)k08305* and $bancal^{w5}$, a deficiency for the region, and found that the resulting heterozygotes have severely malformed legs that resemble those seen in *l(2)k08305* homozygotes. This is consistent with the *P* element being responsible for the mutant phenotype in line *l(2)k08305*.

Identification of candidate genes disrupted by the *l(2)07022* and *l(2)k08305 P*-element insertions: Having determined that the *P* element is responsible for the mutant phenotypes in lines *l(2)07022* and *l(2)k08305*, we set out to identify the gene nearest the insertion site in each line. First, plasmid rescue was used to obtain DNA flanking the insertion site (HAMILTON and ZINN 1994). The sequence of this flanking DNA was then used to BLAST search the BDGP expressed sequence tag (EST) database. The corresponding cDNAs were sequenced, putative open reading frames identified, and the sequence analyzed for similarity to previously identified proteins.

For line *l(2)07022*, a region of ~400 bp from the plasmid rescue fragment was found to be identical to a family of 11 overlapping ESTs in the BDGP database. A cDNA corresponding to a representative of this EST family, LD18846, was sequenced. LD18846 was found to be 2360 bp in length and to contain a predicted open reading frame (ORF) encoding a 605-amino-acid protein (GenBank accession no. AF275628). This ORF is not preceded by in-frame stop codons, suggesting that longer cDNAs may exist. The *l(2)07022 P* element is inserted within the coding region, 711 bp downstream from the putative translation start site. We have named this gene *vulcan* (*vlc*) after the Roman god who broke both his legs as he fell to earth upon being thrown from heaven by Jupiter. Vulcan is ~40% identical over a region of 115 amino acids in its carboxy terminal domain to a family of rat proteins called SAPAPs (TAKEUCHI *et al.* 1997; Figure 4). This carboxy terminal region is also 34–42% identical to a region of a predicted Drosophila protein, a predicted *Caenorhabditis elegans* protein, and a predicted human protein of unknown function (Figure 4). We were unable to identify additional regions of homology to previously identified proteins.

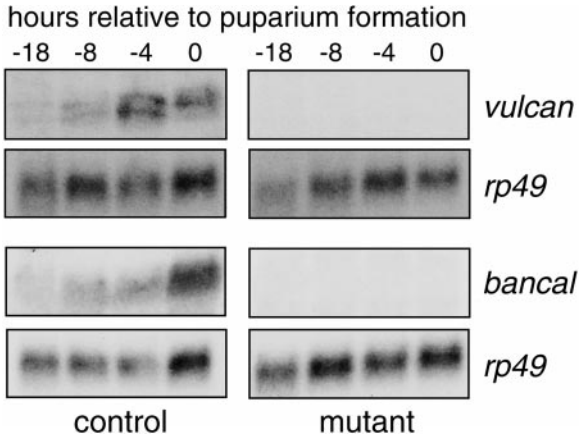

FIGURE 5.—*Vulcan* and *bancal* transcription is undetectable in mutant late third instar larvae and newly formed prepupae. Total RNA isolated from control and homozygous mutant mid- (−18 hr and −8 hr) and late (−4 hr) third instar larvae, as well as newly formed prepupae (0 hr), was fractionated by formaldehyde agarose gel electrophoresis and analyzed by Northern blot hybridization. Two blots were made, one containing RNA from staged *yw* control and homozygous *l(2)07022* animals and the other containing RNA from staged *yw* control and homozygous *l(2)k08305* animals. Radiolabeled probes directed against a portion of the respective cDNA were used to detect either *vulcan* or *bancal* transcription. Each blot was hybridized to detect *rp49* mRNA as a control for loading and transfer.

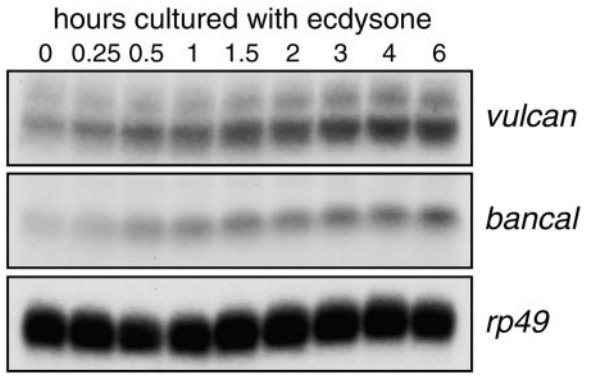

FIGURE 6.—*Vulcan* and *bancal* transcription is inducible by ecdysone. Late third instar larval organs (primarily salivary glands, gut fragments, Malpighian tubules, and imaginal discs) were cultured for the times indicated with 5×10^{-6} M 20-hydroxyecdysone, as described (KARIM and THUMMEL 1991). Total RNA was fractionated by formaldehyde agarose gel electrophoresis and hybridized to detect *vlc* and *bl* RNA. Approximately equal amounts of RNA are present in all lanes, as determined by hybridization to detect *rp49* mRNA.

For line *l(2)k08305*, a region of ~140 bp from the plasmid rescue fragment was found to be 97% identical to a family of 13 overlapping ESTs in the BDGP database. A cDNA corresponding to a representative of this EST family, GM13955, was sequenced. This cDNA is 2028 bp in length and contains a predicted ORF encoding a 508-amino-acid protein (GenBank accession no. AF275629), corresponding to the previously identified Drosophila homologue of hnRNP K, Bancal (CHARROUX *et al.* 1999). The *P* element in line *l(2)k08305* was found to be inserted within the first intron of *bancal* (*bl*), 792 bp downstream from the 5′ splice site.

The disrupted genes are not expressed in *l(2)07022* and *l(2)k08305* mutant third instar larvae: To determine if the *l(2)07022* and *l(2)k08305 P*-element insertions affect *vlc* and *bl* expression, respectively, we examined the transcription of these genes in homozygous mutant animals by Northern blot hybridization. Two RNA size classes, 2.7 and 3 kb in length, were detected by hybridization with a radioactive *vlc* probe in control late third instar larvae and newly formed prepupae (Figure 5). The levels of *vlc* mRNA increase in late third instar larvae, suggesting that this gene may be ecdysone inducible. In addition, there appears to be a temporal switch in the sizes of *vlc* mRNA, because both the 2.7- and 3-kb mRNAs are expressed in late third instar larvae while the larger mRNA predominates at puparium formation (Figure 5). Neither *vlc* transcript is detectable in *l(2)07022* homozygous mutant animals, verifying that *vlc* is the gene disrupted by the *P*-element insertion in line *l(2)07022* (Figure 5). This also suggests that line *l(2)07022* is at least a strong hypomorphic allele of *vlc*.

Northern blot hybrization of RNA isolated from control animals using a *bl* cDNA probe revealed a single mRNA of 2 kb in length (Figure 5). The temporal profile of *bl* transcription is also consistent with it being induced by ecdysone, showing a peak at puparium formation (Figure 5). The *bl* transcript is not detectable in *l(2)k08305* homozygous mutant animals, demonstrating that *bl* is the gene mutated by the *P*-element insertion in this line and that the *l(2)k08305* mutation is at least a strong hypomorphic allele of *bl*.

***vulcan* and *bancal* are rapidly induced by ecdysone in late third instar larval organs:** Both *vlc* and *bl* mRNA increase in abundance at the end of larval development, coincident with the high-titer pulse of ecdysone that triggers puparium formation (Figure 5). This expression profile suggests that these genes may be ecdysone inducible. To test this hypothesis, we examined *vlc* and *bl* transcription in late third instar larval organs that had been cultured for various times in the presence of ecdysone (Figure 6). Transcripts from both genes increase in abundance by 15–30 min after ecdysone addition and continue to accumulate throughout the time course, consistent with these genes being directly induced by the hormone.

DISCUSSION

An enhancer trap screen for ecdysone-inducible genes required for adult leg morphogenesis: Extensive studies have focused on the proliferation and patterning of imaginal discs that occur during larval development in Drosophila (COHEN 1993). In contrast, relatively few

studies have addressed the question of how these patterned discs undergo the remarkable transformation from a folded epithelial monolayer to a mature adult structure. This transformation has been shown to be dependent on changes in ecdysone concentration, indicating that pulses of ecdysone during metamorphosis coordinate the maturation of appropriate adult structures (Fristrom and Fristrom 1993). As might be expected, ecdysone-inducible transcription factors, such as the *BR-C* and *crol*, are required for leg morphogenesis, as are a range of structural genes that encode cytoskeletal and adherens junction components as well as a transmembrane serine protease (von Kalm *et al.* 1995; D'Avino and Thummel 1998). In this article, we describe an enhancer trap screen that was designed to expand the collection of genes that link the ecdysone signal to leg morphogenesis.

This screen identified 12 *P*-element insertion lines that display an increase in *lacZ* expression in late third instar larvae as well as pupal lethality with defects in adult leg development. In all cases, *lacZ* expression is low or absent in leg imaginal discs of mid-third instar larvae, but increases significantly in late third instar larvae in parallel with the high-titer ecdysone pulse that triggers puparium formation. Of these lines, four display an increase in *lacZ* expression in imaginal discs cultured with ecdysone. These lines were subjected to further characterization and resulted in the identification of *vulcan* and *bancal*. Consistent with the regulation of *lacZ* expression in the enhancer trap lines, both *vlc* and *bl* transcription increases dramatically at the onset of metamorphosis (Figure 5). In addition, induction of both genes can be detected within 15–30 min after ecdysone addition, suggesting that they are directly induced by the hormone (Figure 6). These observations indicate that *vlc* and *bl* provide a direct link between the ecdysone signal and the initial steps of ecdysone-triggered leg elongation.

Our future plans include characterization of the remaining eight lines that displayed increased *lacZ* expression in leg imaginal discs of late third instar larvae. The regulation of *lacZ* expression in these lines raises the possibility that the corresponding gene might be a secondary-response target of ecdysone signaling in imaginal discs. Secondary-response genes display little or no ecdysone induction in organ culture, most likely as a result of anoxic stress associated with the culture conditions (G. Lam and C. S. Thummel, unpublished results). Identification of the mutated gene in these lines should provide further insights into the mechanisms by which ecdysone controls adult leg development.

Vulcan may function at the septate junction during leg morphogenesis: One of the ecdysone-inducible genes that we identified as being required for leg disc elongation was *vulcan* (*vlc*). *vlc* mutants die primarily as pharate adults, with short malformed legs (Table 1, Figure 2). The femur and tibia in these mutants are shorter and thicker than wild type, and the distal tarsal segments are short and curved (Figures 2 and 3).

A BLAST search with the predicted Vlc protein revealed a region of sequence similarity with a family of rat proteins called SAPAPs (also known as DAPs and GKAPs). SAPAPs were identified through their ability to interact, in a yeast two-hybrid assay, with the guanylate kinase domain of PSD-95/SAP90 (Kim *et al.* 1997; Satoh *et al.* 1997; Takeuchi *et al.* 1997). PSD-95/SAP90 is a member of the membrane-associated guanylate kinase (MAGUK) family of proteins that is localized to postsynaptic densities within the vertebrate central nervous system (Cho *et al.* 1992; Kistner *et al.* 1993; Hunt *et al.* 1996). MAGUKs share a common domain structure consisting of one or three PDZ (*P*SD-95/SAP90, *D*iscs-large, *Z*O-1) domains, an SH3 (Src-homology 3) domain, and a domain with homology to yeast guanylate kinase. Each of these domains has been shown to mediate protein-protein interactions, allowing MAGUKs to function as molecular scaffolds that bring multiple proteins together at specialized regions of the plasma membrane (Dimitratos *et al.* 1999). PSD-95/SAP90 has not only been shown to bind SAPAPs through its guanylate kinase domain, but also the *N*-methyl-D-aspartate receptor (Kornau *et al.* 1995), Shaker-type potassium channels (Kim *et al.* 1995), and neuronal nitric oxide synthase (Brenman *et al.* 1996) through its PDZ domains. While SAPAPs have subsequently been shown to colocalize with and bind to PSD-95/SAP90 *in vivo* (Kim *et al.* 1997; Satoh *et al.* 1997), no studies have yet determined their function at postsynaptic densities.

There are three known MAGUK family members in Drosophila: *discs-large* (*dlg*; Woods and Bryant 1991), *camguk* (*cam*; Dimitratos *et al.* 1997), and *polychaetoid* (*pyd*, also known as *tamou*; Takahisa *et al.* 1996). Of these, Dlg is most closely related to PSD-95/SAP90, with 52–67% amino acid identity within the PDZ and SH3 interaction domains and 67% identity within the guanylate kinase (GUK) domains (Woods and Bryant 1993). Since Vlc shares sequence similarity with SAPAPs and SAPAPs bind to the GUK domain of PSD-95/SAP90, it is possible that Vlc interacts with the GUK domain of Dlg. To test this hypothesis, we looked for dominant genetic interactions between either the *vlc P*-element allele (vlc^{07022}) or deficiency (*Df(2R)M41A4*) and six different *dlg* alleles (*m52*, *G3*, *m30*, *IP20*, *v59*, *v55*). These *dlg* alleles include genetic and molecular nulls as well as hypomorphs that produce truncated proteins lacking portions of the GUK domain (Woods *et al.* 1996). Although we did not observe a dominant genetic interaction with any of these alleles (data not shown), we plan to look for recessive genetic interactions as well as determine whether Vlc and Dlg proteins can directly bind to one another.

The Dlg protein is localized to the cytoplasmic face of the septate junction in imaginal disc cells (Woods *et al.* 1996). The septate junction is positioned just basal

to the adherens junction and has been proposed to be functionally analogous to the vertebrate tight junction (Woods and Bryant 1993). In *dlg* null mutants, septate junctions are not maintained, resulting in defective cell-cell adhesion, a loss of cell polarity, and unregulated cell proliferation (Woods *et al.* 1996). If Vlc interacts with Dlg in the region of the septate junction, then Vlc may function to maintain proper intercellular adhesion or cell polarity during leg elongation. A role for septate junction-associated proteins during epithelial morphogenesis is not unprecedented. Both the Drosophila homologue of protein 4.1, Coracle (Fehon *et al.* 1994), and Neurexin (Baumgartner *et al.* 1996) localize to the septate junction. Mutations in these genes result in animals that die as embryos with defects in the morphogenetic process of dorsal closure. A function for septate junction-associated proteins during imaginal disc morphogenesis, however, has not yet been established.

Recent studies have also shown that *vlc* mutations can interact with mutations in the nonmuscle myosin II heavy chain gene, *zipper* (*zip*). Mutations in *zip* limit cell shape changes and thereby lead to defective leg elongation (von Kalm *et al.* 1995). In addition, a *zip* allele was isolated as enhancer of the malformed leg phenotype in *broad*^{1} mutants, indicating that it functions in the ecdysone signaling pathway that controls leg morphogenesis (Gotwals and Fristrom 1991). Interestingly, a deficiency that removes *vlc* also shows a weak genetic interaction with *zip* (10–24% malformed legs; Halsell and Kiehart 1998). Later studies showed a similar degree of interaction with the *l(2)07022 P*-element insertion in *vlc* (S. Halsell, personal communication). It is thus possible that Vlc exerts at least some of its effects on leg morphogenesis through interactions with Zip and/or other components of the apical contractile belt. Further studies of *vlc* may provide the first indication that septate junctions are critical for the cell shape changes that drive leg disc elongation as well as provide insight into how the ecdysone signal triggers the cell shape changes associated with leg morphogenesis.

Bancal may regulate genes that direct adult leg morphogenesis: The second ecdysone-inducible gene that we identified as required for leg disc elongation was *bancal* (*bl*). *bl* mutants die primarily as pupae and pharate adults, with short malformed legs (Table 1, Figure 2). The femur and tibia in these mutants are significantly shorter and thicker than wild type with a distinct kink in the femur and a short thick basi-tarsus (Figures 2 and 3). Recently, Charroux *et al.* (1999) suggested that the malformed legs observed in *bl* mutants are a result of reduced cell proliferation in third instar imaginal discs. While it is possible that a reduction in cell proliferation may contribute to this phenotype, our results indicate that the malformed legs of *bl* mutant animals are primarily caused by defects in leg morphogenesis during the onset of metamorphosis (Table 2). Charroux *et al.* (1999) also showed that the wings of *bl* mutants display the classic broad phenotype, suggesting defects in wing morphogenesis (Gotwals and Fristrom 1991; von Kalm *et al.* 1995).

bancal encodes the Drosophila homolog of hnRNP K. hnRNPs are RNA binding proteins that perform a wide range of functions in the cell, including splicing regulation, mRNA transport, mRNA stability, and translational silencing (Dreyfuss *et al.* 1993; Krecic and Swanson 1999). hnRNP K is considered an atypical hnRNP in that it binds nucleic acids through three KH domains (Siomi *et al.* 1993, 1994) rather than the RNA-binding consensus sequence used by most other hnRNPs (Dreyfuss *et al.* 1993). One function of this RNA binding activity is to suppress translation, as hnRNP K has been shown to directly silence 15-lipoxygenase and human papillomavirus L2 translation by binding to specific inhibitory elements in these mRNAs (Ostareck *et al.* 1997; Collier *et al.* 1998). hnRNP K can also bind to single-stranded DNA in a sequence-specific manner, recognizing C-rich regions (Gaillard *et al.* 1994; Ito *et al.* 1994; Ostrowski *et al.* 1994; Tomonaga and Levens 1995; Michelotti *et al.* 1996). *In vitro* transcription assays and tissue culture transfection studies indicate that hnRNP K can function through these C-rich regions to activate or repress transcription (Michelotti *et al.* 1996; Du *et al.* 1998).

On the basis of these functions for hnRNP K in vertebrate systems, we propose that Bancal may regulate the transcription or translation of ecdysone-inducible genes required for leg morphogenesis in Drosophila. This proposal is supported by a weak genetic interaction we have observed between *bl* alleles and the *broad*^{1} allele of the *BR-C* (J. Gates and C. S. Thummel, unpublished results). We plan to examine *BR-C* mRNA and protein levels in *bl* mutant third instar larvae and prepupae. In addition, there is a switch in *BR-C* mRNA isoforms that occurs in imaginal discs at puparium formation, which may, at least in part, be regulated at the level of splicing (Emery *et al.* 1994; Bayer *et al.* 1996). Since hnRNP K can bind RNA, Bancal could facilitate the *BR-C* isoform switch by reducing the stability of some mRNAs or by effecting a temporal change in splice site choice. We can test these models by characterizing different *BR-C* mRNA isoforms in wild-type and *bl* mutant animals. In addition, we plan to examine the expression of other ecdysone-regulated genes required for adult leg morphogenesis, including *Sb* (Appel *et al.* 1993), *E74* (Fletcher *et al.* 1995), β*FTZ-F1* (Broadus *et al.* 1999), and *crol* (D'Avino and Thummel 1998), in a *bl* mutant background. These studies should indicate whether ecdysone-induced *bl* expression at puparium formation contributes to the cascade of gene expression that regulates the eversion and elongation of leg imaginal discs.

The ability of hnRNP K to interact with DNA, RNA, and other proteins in the hnRNP particle has led to the proposal that this factor is involved in bridging multicomponent regulatory systems (Bomsztyk *et al.* 1997;

Ostareck-Lederer *et al.* 1998). This proposed widespread function for hnRNP K, however, contrasts with the relatively specific effect of *bl* mutations on the morphogenesis of adult imaginal disc derivatives. It seems likely that further functional characterization of *bl* function in Drosophila may not only shed light on the hormonal regulation of adult leg morphogenesis but may also provide new insights into the regulatory functions of hnRNP K in other organisms.

We thank T. Laverty and G. Rubin for providing the collection of *P*-element insertions on the second chromosome prior to publication, P. Bryant and S. Kerridge for providing mutant stocks, J. Roote for help and advice in characterizing *l(2)05271*, G. Panganiban for Dll antibody, T. Orenic and R. Holmgren for Ci antibody, L. von Kalm for many insightful conversations, and R. Ward and T. Kozlova for critical comments on the manuscript. J.G. is a Predoctoral Fellow and C.S.T. is an Investigator with the Howard Hughes Medical Institute.

LITERATURE CITED

Andres, A. J., and C. S. Thummel, 1994 Methods for quantitative analysis of transcription in larvae and prepupae. Methods Cell Biol. **44:** 565–573.

Appel, L. F., M. Prout, R. Abu-Shumays, A. Hammonds, J. C. Garbe *et al.*, 1993 The *Drosophila Stubble-stubbloid* gene encodes an apparent transmembrane serine protease required for epithelial morphogenesis. Proc. Natl. Acad. Sci. USA **90:** 4937–4941.

Baumgartner, S., J. T. Littleton, K. Broadie, M. A. Bhat, R. Harbecke *et al.*, 1996 A *Drosophila neurexin* is required for septate junction and blood-nerve barrier formation and function. Cell **87:** 1059–1068.

Bayer, C. A., B. Holley and J. W. Fristrom, 1996 A switch in *broad-complex* zinc-finger isoform expression is regulated posttranscriptionally during the metamorphosis of *Drosophila* imaginal discs. Dev. Biol. **177:** 1–14.

Beaton, A. H., I. Kiss, D. Fristrom and J. W. Fristrom, 1988 Interaction of the *Stubble-stubbloid* locus and the *Broad-complex* of *Drosophila melanogaster*. Genetics **120:** 453–464.

Bomsztyk, K., I. V. Seuningen, H. Suzuki, O. Denisenko and J. Ostrowski, 1997 Diverse molecular interactions of the hnRNP K protein. FEBS Lett. **403:** 113–115.

Brenman, J. E., D. S. Chao, S. H. Gee, A. W. McGee, S. E. Craven *et al.*, 1996 Interaction of nitric oxide synthase with the postsynaptic density protein PSD-95 and alpha1-syntrophin mediated by PDZ domains. Cell **84:** 757–767.

Broadus, J., J. R. McCabe, B. Endrizzi, C. S. Thummel and C. T. Woodard, 1999 The *Drosophila* βFTZ-F1 orphan nuclear receptor provides competence for stage-specific responses to the steroid hormone ecdysone. Mol. Cell **3:** 143–149.

Charroux, B., C. Angelats, L. Fasano, S. Kerridge and C. Vola, 1999 The levels of the *bancal* product, a *Drosophila* homologue of vertebrate hnRNP K protein, affect cell proliferation and apoptosis in imaginal disc cells. Mol. Cell. Biol. **19:** 7846–7856.

Cho, K. O., C. A. Hunt and M. B. Kennedy, 1992 The rat brain postsynaptic density fraction contains a homologue of the *Drosophila* Discs-large tumor suppressor protein. Neuron **9:** 929–942.

Clark, H. F., D. Brentrup, K. Schneitz, A. Bieber, C. Goodman *et al.*, 1995 *Dachsous* encodes a member of the cadherin superfamily that controls imaginal disc morphogenesis in *Drosophila*. Genes Dev. **9:** 1530–1542.

Cohen, S. M., 1993 Imaginal disc development, pp. 747–841 in *The Development of Drosophila melanogaster*, edited by M. Bate and A. Martinez-Arias. Cold Spring Harbor Laboratory Press, Cold Spring Harbor, NY.

Collier, B., L. Goobar-Larsson, M. Sokolowski and S. Schwartz, 1998 Translational inhibition *in vitro* of human papillomavirus type 16 L2 mRNA mediated through interaction with heterogeneous ribonucleoprotein K and poly(rC)-binding proteins 1 and 2. J. Biol. Chem. **273:** 22648–22656.

Condic, M. L., D. Fristrom and J. W. Fristrom, 1991 Apical cell shape changes during *Drosophila* imaginal leg disc elongation: a novel morphogenetic mechanism. Development **111:** 23–33.

D'Avino, P. P., and C. S. Thummel, 1998 *crooked legs* encodes a family of zinc finger proteins required for leg morphogenesis and ecdysone-regulated gene expression during *Drosophila* metamorphosis. Development **125:** 1733–1745.

Dimitratos, S. D., D. F. Woods and P. J. Bryant, 1997 Camguk, Lin-2, and CASK: novel membrane-associated guanylate kinase homologs that also contain CaM kinase domains. Mech. Dev. **63:** 127–130.

Dimitratos, S. D., D. F. Woods, D. G. Stathakis and P. J. Bryant, 1999 Signaling pathways are focused at specialized regions of the plasma membrane by scaffolding proteins of the MAGUK family. Bioessays **21:** 912–921.

Dreyfuss, G., M. J. Matunis, S. Pinol-Roma and C. G. Burd, 1993 hnRNP proteins and the biogenesis of mRNA. Annu. Rev. Biochem. **62:** 289–321.

Du, Q., I. N. Melnikova and P. D. Gardner, 1998 Differential effects of heterogeneous nuclear ribonucleoprotein K on Sp1- and Sp3-mediated transcriptional activation of a neuronal nicotinic acetylcholine receptor promoter. J. Biol. Chem. **273:** 19877–19883.

Edwards, K. A., and D. P. Kiehart, 1996 *Drosophila nonmuscle myosin II* has multiple essential roles in imaginal disc and egg chamber morphogenesis. Development **122:** 1499–1511.

Emery, I. F., V. Bedian and G. M. Guild, 1994 Differential expression of *Broad-Complex* transcription factors may forecast tissue-specific developmental fates during *Drosophila* metamorphosis. Development **120:** 3275–3287.

Fehon, R. G., I. A. Dawson and S. Artavanis-Tsakonas, 1994 A *Drosophila* homologue of membrane-skeleton protein 4.1 is associated with septate junctions and is encoded by the *coracle* gene. Development **120:** 545–557.

Fekete, E., D. Fristrom, I. Kiss and J. W. Fristrom, 1975 The mechanism of evagination of imaginal discs of *Drosophila melanogaster*. II. Studies on trypsin-accelerated evagination. Roux's Arch. Dev. Biol. **173:** 123–138.

Fletcher, J. C., K. C. Burtis, D. S. Hogness and C. S. Thummel, 1995 The *Drosophila E74* gene is required for metamorphosis and plays a role in the polytene chromosome puffing response to ecdysone. Development **121:** 1455–1465.

Fristrom, D., and J. W. Fristrom, 1975 The mechanism of evagination of imaginal discs of *Drosophila melanogaster*. I. General considerations. Dev. Biol. **43:** 1–23.

Fristrom, D., and J. W. Fristrom, 1993 The metamorphic development of the adult epidermis, pp. 843–897 in *The Development of Drosophila melanogaster*, edited by M. Bate and A. Martinez-Arias. Cold Spring Harbor Laboratory Press, Cold Spring Harbor, NY.

Gaillard, C., E. Cabannes and F. Strauss, 1994 Identity of the RNA-binding protein K of hnRNP particles with protein H16, a sequence-specific single strand DNA-binding protein. Nucleic Acids Res. **22:** 4183–4186.

Geiger, B., and O. Ayalon, 1992 Cadherins. Annu. Rev. Cell Biol. **8:** 307–332.

Gotwals, P. J., and J. W. Fristrom, 1991 Three neighboring genes interact with the *Broad-Complex* and the *Stubble-stubbloid* locus to affect imaginal disc morphogenesis in *Drosophila*. Genetics **127:** 747–759.

Halsell, S. R., and D. P. Kiehart, 1998 Second-site noncomplementation identifies genomic regions required for *Drosophila* nonmuscle myosin function during morphogenesis. Genetics **148:** 1845–1863.

Hamilton, B. A., and K. Zinn, 1994 From clone to mutant gene. Methods Cell Biol. **44:** 81–94.

Hunt, C. A., L. J. Schenker and M. B. Kennedy, 1996 PSD-95 is associated with the postsynaptic density and not with the presynaptic membrane at forebrain synapses. J. Neurosci. **16:** 1380–1388.

Ito, K., K. Sato and H. Endo, 1994 Cloning and characterization of a single-stranded DNA binding protein that specifically recognizes deoxycytidine stretch. Nucleic Acids Res. **22:** 53–58.

Karim, F. D., and C. S. Thummel, 1991 Ecdysone coordinates the timing and amounts of *E74A* and *E74B* transcription in *Drosophila*. Genes Dev. **5:** 1067–1079.

Karpen, G. H., and A. C. Spradling, 1992 Analysis of subtelomeric

heterochromatin in the *Drosophila* minichromosome Dp1187 by single P element insertional mutagenesis. Genetics **132:** 737–753.

Kim, E., M. Niethammer, A. Rothschild, Y. N. Jan and M. Sheng, 1995 Clustering of Shaker-type K+ channels by interaction with a family of membrane-associated guanylate kinases. Nature **378:** 85–88.

Kim, E., S. Naisbitt, Y. P. Hsueh, A. Rao, A. Rothschild *et al.*, 1997 GKAP, a novel synaptic protein that interacts with the guanylate kinase-like domain of the PSD-95/SAP90 family of channel clustering molecules. J. Cell Biol. **136:** 669–678.

Kiss, I., A. H. Beaton, J. Tardiff, D. Fristrom and J. W. Fristrom, 1988 Interactions and developmental effects of mutations in the *Broad-Complex* of *Drosophila melanogaster*. Genetics **118:** 247–259.

Kistner, U., B. M. Wenzel, R. W. Veh, C. Cases-Langhoff, A. M. Garner *et al.*, 1993 SAP90, a rat presynaptic protein related to the product of the *Drosophila* tumor suppressor gene *dlg-A*. J. Biol. Chem. **268:** 4580–4583.

Kornau, H. C., L. T. Schenker, M. B. Kennedy and P. H. Seeburg, 1995 Domain interaction between NMDA receptor subunits and the postsynaptic density protein PSD-95. Science **269:** 1737–1740.

Krecic, A. M., and M. S. Swanson, 1999 hnRNP complexes: composition, structure, and function. Curr. Opin. Cell Biol. **11:** 363–371.

Michelotti, E. F., G. A. Michelotti, A. I. Aronsohn and D. Levens, 1996 Heterogeneous nuclear ribonucleoprotein K is a transcription factor. Mol. Cell. Biol. **16:** 2350–2360.

Motzny, C. K., and R. Holmgren, 1995 The *Drosophila* Cubitus interruptus protein and its role in the *wingless* and *hedgehog* signal transduction pathways. Mech. Dev. **52:** 137–150.

Ostareck, D. H., A. Ostareck-Lederer, M. Wilm, B. J. Thiele, M. Mann *et al.*, 1997 mRNA silencing in erythroid differentiation: hnRNP K and hnRNP E1 regulate 15-lipoxygenase translation from the 3′ end. Cell **89:** 597–606.

Ostareck-Lederer, A., D. H. Ostareck and M. W. Hentze, 1998 Cytoplasmic regulatory functions of the KH-domain proteins hnRNPs K and E1/E2. Trends Biochem. Sci. **23:** 409–411.

Ostrowski, J., I. Van Seuningen, R. Seger, C. T. Rauch, P. R. Sleath *et al.*, 1994 Purification, cloning, and expression of a murine phosphoprotein that binds the kappa B motif *in vitro* identifies it as the homolog of the human heterogeneous nuclear ribonucleoprotein K protein. Description of a novel DNA-dependent phosphorylation process. J. Biol. Chem. **269:** 17626–17634.

Panganiban, G., A. Sebring, L. Nagy and S. Carroll, 1995 The development of crustacean limbs and the evolution of arthropods. Science **270:** 1363–1366.

Pino-Heiss, S., and G. Schubiger, 1989 Extracellular protease production by *Drosophila* imaginal discs. Dev. Biol. **132:** 282–291.

Poodry, C. A., and H. A. Schneiderman, 1971 Intercellular adhesivity and pupal morphogenesis in *Drosophila melanogaster*. Roux's Arch. Dev. Biol. **168:** 1–9.

Satoh, K., H. Yanai, T. Senda, K. Kohu, T. Nakamura *et al.*, 1997 DAP-1, a novel protein that interacts with the guanylate kinase-like domains of hDLG and PSD-95. Genes Cells **2:** 415–424.

Siomi, H., M. J. Matunis, W. M. Michael and G. Dreyfuss, 1993 The pre-mRNA binding K protein contains a novel evolutionarily conserved motif. Nucleic Acids Res. **21:** 1193–1198.

Siomi, H., M. Choi, M. C. Siomi, R. L. Nussbaum and G. Dreyfuss, 1994 Essential role for KH domains in RNA binding: impaired RNA binding by a mutation in the KH domain of FMR1 that causes fragile X syndrome. Cell **77:** 33–39.

Spradling, A. C., D. M. Stern, I. Kiss, J. Roote, T. Laverty *et al.*, 1995 Gene disruptions using P transposable elements: an integral component of the *Drosophila* genome project. Proc. Natl. Acad. Sci. USA **92:** 10824–10830.

Spradling, A. C., D. Stern, A. Beaton, E. J. Rhem, T. Laverty *et al.*, 1999 The Berkeley *Drosophila* Genome Project gene disruption project: single *P*-element insertions mutating 25% of vital Drosophila genes. Genetics **153:** 135–177.

Takahisa, M., S. Togashi, T. Suzuki, M. Kobayashi, A. Murayama *et al.*, 1996 The *Drosophila tamou* gene, a component of the activating pathway of *extramacrochaetae* expression, encodes a protein homologous to mammalian cell-cell junction-associated protein ZO-1. Genes Dev. **10:** 1783–1795.

Takeuchi, M., Y. Hata, K. Hirao, A. Toyoda, M. Irie *et al.*, 1997 SAPAPs: a family of PSD-95/SAP90-associated proteins localized at postsynaptic density. J. Biol. Chem. **272:** 11943–11951.

Tomonaga, T., and D. Levens, 1995 Heterogeneous nuclear ribonucleoprotein K is a DNA-binding transactivator. J. Biol. Chem. **270:** 4875–4881.

Torok, T., G. Tick, M. Alvarado and I. Kiss, 1993 P-lacW insertional mutagenesis on the second chromosome of *Drosophila melanogaster*: isolation of lethals with different overgrowth phenotypes. Genetics **135:** 71–80.

von Kalm, L., D. Fristrom and J. Fristrom, 1995 The making of a fly leg: a model for epithelial morphogenesis. Bioessays **17:** 693–702.

Woods, D. F., and P. J. Bryant, 1991 The *discs-large* tumor suppressor gene of *Drosophila* encodes a guanylate kinase homolog localized at septate junctions. Cell **66:** 451–464.

Woods, D. F., and P. J. Bryant, 1993 ZO-1, DlgA and PSD-95/SAP90: homologous proteins in tight, septate and synaptic cell junctions. Mech. Dev. **44:** 85–89.

Woods, D. F., C. Hough, D. Peel, G. Callaini and P. J. Bryant, 1996 Dlg protein is required for junction structure, cell polarity, and proliferation control in *Drosophila* epithelia. J. Cell Biol. **134:** 1469–1482.

Young, P. E., A. M. Richman, A. S. Ketchum and D. P. Kiehart, 1993 Morphogenesis in *Drosophila* requires nonmuscle myosin heavy chain function. Genes Dev. **7:** 29–41.

Communicating editor: S. Henikoff